water

MDPI

Article

Efficient Removal of Methyl Red Dye by Using Bark of Hopbush

Salma Gul [1], Mansha Kanwal [1], Raina Aman Qazi [2], Hajera Gul [2], Rozina Khattak [2,*], Muhammad Sufaid Khan [3], Fatima Khitab [2] and Andrey E. Krauklis [4]

[1] Department of Chemistry, Women University Swabi, Swabi 22101, Pakistan
[2] Department of Chemistry, Shaheed Benazir Bhutto Women University, Peshawar 25000, Pakistan
[3] Department of Chemistry, University of Malakand, Chakdara 18800, Pakistan
[4] Institute for Mechanics of Materials, University of Latvia, Jelgavas Street 3, LV-1004 Riga, Latvia
* Correspondence: rznkhattak@sbbwu.edu.pk or rznkhattak@yahoo.com

Highlights:

- Analysis of low-cost, bio-adsorbent bark of the *D. viscosa* plant, proved to be an efficient adsorbent for the removal of methyl red dye from aqueous solution.
- The pseudo-second-order kinetic model and Freundlich adsorption isotherm appeared to be the best fit for describing the adsorption of methyl red onto *D. viscosa* plant bark.
- *D. viscosa* plant bark as an adsorbent showed good adsorption capability in tap water and river water.

Abstract: Methyl red (MR) dye, one of the azo dyes, is mutagenic and its persistence has negative effects on the environment and people's health. The current work is the first to demonstrate that methyl red dye can be removed effectively and sustainably, utilizing biomass derived from the bark of the *Dodonaea viscosa* (Hopbush) plant. The Hopbush bark shows effective adsorption of MR, upto 73%, under optimized conditions in an aqueous medium. The experimental conditions were optimized by examining the effect of time, initial dye concentration, pH and ionic strength on the adsorption process in an aqueous medium. Maximum (i.e., 73%) adsorption of MR removal (500 ppm) was observed in highly acidic conditions (pH = 1) at a contact time of 75 min. The pseudo-second-order kinetic model and Freundlich adsorption isotherm appeared to be the most appropriate for characterizing the MR's adsorption onto the bark of the *D. viscosa* plant. Furthermore, it was shown that bark powder outperformed animal charcoal, silica gel, and powdered flowers, as well as the leaves of the same species, in terms of adsorption capacity. Thus, a natural adsorbent that is inexpensive and readily available—the bark of the *D. viscosa* plant—can be used to effectively remove harmful dyes from contaminated water and protect water resources from harmful pollutants.

Keywords: *Dodonaea viscosa* plant bark; animal charcoal; silica gel; adsorption kinetics; adsorption isotherm

check for updates

Citation: Gul, S.; Kanwal, M.; Qazi, R.A.; Gul, H.; Khattak, R.; Khan, M.S.; Khitab, F.; Krauklis, A.E. Efficient Removal of Methyl Red Dye by Using Bark of Hopbush. *Water* **2022**, *14*, 2831. https://doi.org/10.3390/w14182831

Academic Editor: Antonio Zuorro

Received: 8 August 2022
Accepted: 5 September 2022
Published: 11 September 2022

1. Introduction

All living things need water to survive. Animals and birds, as well as humans, depend on clean water for survival. The water bodies become contaminated over time. When waste is dumped into water directly or when noxious chemicals and microorganisms enter water bodies, water pollution occurs. Water-related illnesses claim the lives of more than 5 million people annually, which is approximately 10 times as many as are killed in wars. Two-thirds of the world's population is predicted to reside in nations with moderate to severe water shortages by 2025 [1]. Due to water pollution brought on by various human activities, particularly industrial pollutants, just 0.01 percent of the 3% of pure water on Earth may be utilized for human consumption[2]. The most significant cause of water pollution (from several chemical kinds, the others of which have been excluded from this study), from the perspective of wastewater treatment, is dyes.

Dyes are colored organic compounds, mainly used in the textile, dyeing, tannery, paper, pulp, and paint industries. Their effluents include various dyes, similar to those from dye-manufacturing facilities, which cause numerous ecological issues [3]. Azo dyes are the most prevalent of these dyes [4]. If these dyes are ingested through water, they can result in neurochemical issues, allergies, infections of the eyes or skin, or irritations [4,5]. For the removal of dyes, a variety of treatment techniques are used, including ion exchange, biological treatment, photocatalytic degradation, coagulation, etc. [6]. However, each of them has its own limitations. Ion exchange, for instance, is non-selective, sensitive to pH, and unable to handle highly-concentrated wastewater, while biological treatment takes a very long time to complete the decolorization and fermentation processes, needs a lot of space, and is less adaptable [7]. Unlike coagulation—which uses coagulants that are typically non-biodegradable and monomers that have neurotoxic and cancerous consequences—photocatalytic degradation requires an effective photocatalyst and controlled circumstances, making the procedure very expensive. Adsorption is one of the most efficient, cost-effective, and well-known processes for treating wastewater; as a result, it is frequently used to remove dyes from wastewater [6].

Organic substances with the functional group RN=NR′, in which R and R′ are typically aryl, are known as azo dyes. They are a family of commercially-significant azo compounds, or substances with the bond C-N=N-C. Methyl red (MR) is a mono-azo dye with a (—N=N—) linkage, which is used in the production of textiles and other commercial goods [8]. If ingested or inhaled, it might irritate the pharynx or digestive tract and induce skin and ocular sensitivities [9,10]. Additionally, MR undergoes bioconversion into 2-aminobenzoic acid and N-N-dimethyl-p-phenylene diamine in environments where oxygen is present, because it is mutagenic [11,12]. Many scientists, including Rajoriya et al. [13], Xiang et al. [14], Dawadi et al. [15], Santhi et al. [16] and Mahmoud et al. [17], have tried to discover a means by which to remove MR dye from water before releasing it into recipient water bodies. Numerous bio-materials have been described as adsorbents in the literature, including plant leaves [18–20], chitosan and chitin [20,21], crab shells [22], nutshells [22,23], fruit pods [24,25], egg shells [26,27], fruit shells [28], agricultural wastes [29–31], fish scales [32–34], and various others [35–39]. Plant barks are one of the most often employed adsorbents in investigations involving the removal of contaminants from aqueous environments. Numerous investigations have been conducted in this area [40]. Eucalyptus [41,42], flamboyant pod [43], African border [44], pine [45], Sycamore [46], Azollapinnata [47], and many more plant species are among those researched. Plant barks can be used as adsorbents for water treatment because they are inexpensive and have a number of other benefits as well. Biomaterial-based adsorbents are less labor-intensive, as well as being environmentally benign, and renewable [42,48]. Plant bark has the ability to absorb wastewater contaminants on nonliving cells by extracellular and intracellular accumulation through mild forces of contact, similar to the majority of other plant-based biomaterials. They are suitable as an adsorbent for the desired adsorption process, as a result [49].

Bark from the *D. viscosa* plant was used as an adsorbent in this study to remove MR dye. Common names for this evergreen plant with a quick growth rate include Hopbush and Sanatha. It is both wild and ornamental, and wind and bees are among its pollinators. It thrives in environments with temperatures between 18 and 38 degrees Celsius, although it can even withstand conditions between 7 and 45 degrees Celsius [50]. The *D. viscosa* plant, which is often found in mountainous locations, was collected in the wild, in the Swabi district of Pakistan’s Khyber Pakhtun Khwa (KPK). To maximize the rate of MR adsorption, the adsorption kinetics was studied, and the impact of pH, concentration, contact time, and ionic strength was examined. The adsorption isotherm was also determined in order to understand the adsorption process on our chosen adsorbent. The adsorbent demonstrated outstanding dye-removal efficiency. Additionally, it demonstrated strong MR dye adsorption capacity in both tap water and river water. By using the bark of the *D. viscosa* tree as an effective adsorbent, which can also be utilized directly for the treatment of wastewater released from various industries containing MR, this work intends to protect aquatic bodies from pollution caused by dyes from industrial effluents.

2. Materials and Methods

Methyl Red dye, which was used as an adsorbate in this study, is commonly used as an indicator (see Supplementary Materials: Text E1 and Figures S1 and S2). The adsorbent used was the bark of the *D. viscosa* plant. All the solutions were prepared in distilled water. To maintain the pH of the MR dye solution, 0.5 M hydrochloric acid (Merck) and 0.5 M sodium hydroxide (KOSDAQ listed company, Korea) solutions were used. For comparative study, distilled water, tap water, and river water were used. The sample water was collected from a canal in Hamlet district, Swabi, Pakistan. Sodium chloride salt was also used to check the ionic effect of salt on the rate of adsorption.

The bark from the plant was taken and washed with distilled water five times and then completely dried in the sunlight. After that, the bark was ground into powdery form (Figure 1). The leaves and flowers were also washed with distilled water and then dried and ground, following the same process as used for the bark of the *D. viscosa* plant. The *D. viscosa* used in this research was wild, as shown in Figure 1, wherein (a) shows the complete appearance of the plant, (b) shows the bark of the plant, and (c) shows the powdered bark used during experiments. The 500 ppm solution of MR was prepared by dissolving MR in water after shaking at 298 rpm for 40 min. To find the wavelength maximum (λ_{max}), the absorbance of the stock solution of adsorbate was noted in the wavelength range of 380–465 nm. According to Figure S3 (see Supplementary Materials), the wavelength; 433 nm shows maximum absorption. Therefore, further experiments were carried out at 433 nm to record a time–course graph, showing decrease in absorbance as a function of time. The batch experiment was performed by adding 100 mg of adsorbent to the 10 mL solution of MR dye under continuous stirring (298 rpm), at room temperature (25 °C), and the adsorbent was removed by centrifugation after adsorption. A series of experiments was performed to investigate the effect of the different parameters: pH; initial dye concentration; contact time; and ionic strength; on the adsorption of MR. The value of the amount adsorbed or adsorption capacity; Qe was identified by Equation (1) [51,52].

$$\mathrm{Qe} = \frac{(Ci - Ce)V}{W} \tag{1}$$

Ci is the initial concentration, Ce is the final or equilibrium concentration, V is the total volume of solution taken, and W is the amount of adsorbent used.

The percent removal of the adsorbate was determined by Equation (2) [52].

$$\%\ \text{removal} = \frac{Ci - Ce}{Ci} \times 100 \tag{2}$$

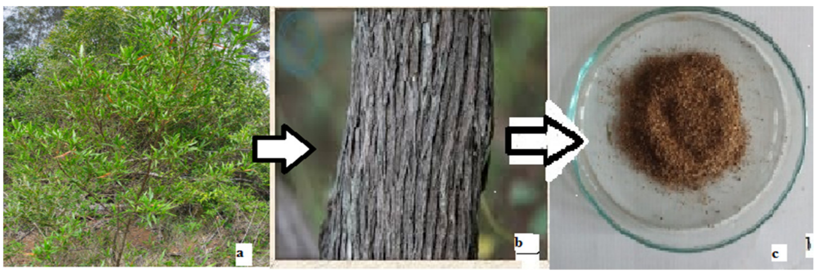

Figure 1. *D. viscosa* plant. (**a**) Plant (**b**) bark of plant (**c**) powdered bark.

Characterizations

Various instruments were used during the study. A digital orbital shaker was used to ensure full mixing of biosorbent and dyes at 298 rpm at room temperature (a product of PCSIR, Islamabad, Pakistan), while centrifugation was carried out at 1000 rpm for 50 min

(Centrifuge 80-2, Changzhou, China). The absorbance was measured by the UV-visible spectrophotometer (Model UV 3000, Hamburg, Germany).

3. Results and Discussion

3.1. Effect of pH on Adsorption

The solution of 500 ppm concentration was prepared and divided into ten beakers. The total volume of each solution was 10 mL. Each solution was maintained at a different pH, at a value between 1 and 10, i.e., beaker 1: pH = 1 and beaker 10: pH = 10, by using 0.5 M HCl (for acidic pH, i.e., from pH 1–6) and 0.5 M NaOH (for basic pH). A total of 100 mg adsorbent (bark of *D. viscosa* plant) was added to each solution, to check the effect of pH on adsorption. The adsorption capacity was determined and plotted against the pH profile. Figure 2 shows the relationship of pH to the adsorption capacity of the adsorbent (Qe). The adsorption capacity decreased with increasing pH and with lowering the strength of protons. At pH = 1, where the adsorption capacity was high (i.e., 34 mg/g), the greatest adsorption was observed. The adsorption capacity declined markedly from pH = 2 (23 mg/g) to pH = 3 (e.g., 8 mg/g), then decreased noticeably less, until pH = 9 (e.g., from 8 mg/g to 2.5 mg/g), before remaining constant at pH = 10. The gradual decrease in the adsorption capacity of bark may be due to electrostatic attraction in the negatively charged dye and the positively charged surface of the adsorbent at pH 1–6. When the pH of the solution increases, it results in an increased number of hydroxyl groups; hence the number of positively charged sites decreases and results in less electrostatic attraction between charges of adsorbate and surface area of adsorbent [12]. Further research was conducted at pH = 1, where the adsorbent's adsorption capacity was at its highest, in order to follow the maximum adsorption rate in the shortest amount of time possible.

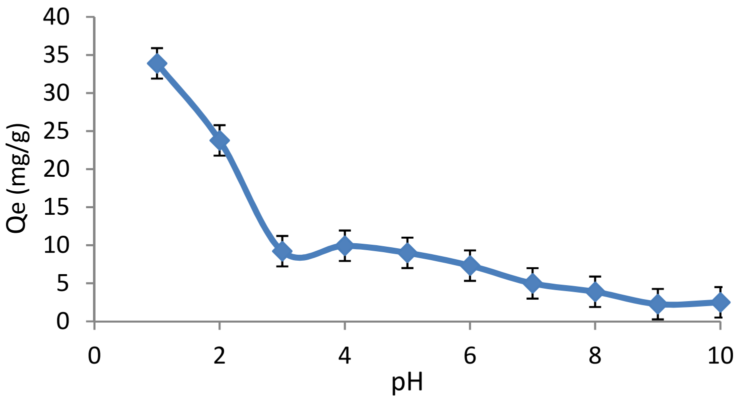

Figure 2. Effect of pH on the adsorption of MR onto *D. viscosa* plant bark.

3.2. Effect of Concentration of MR Dye on Adsorption

Using the standard dilution formula, solutions of MR at various concentrations (ranging from 20 ppm to 560 ppm) were prepared from a stock solution (600 ppm). HCl solution (0.5 M) kept the liquids' pH at 1. The *D. viscosa* bark powder (100 mg) was added to each solution. The solutions were shaken for 60 min at 298 rpm and the suspended adsorbent was separated from the solution by centrifugation. Figure 3 illustrates the relationship between the increasing MR concentrations and the adsorption capacity (Qe) of the adsorbent we chose. Figure 3 demonstrates that as the initial concentration of the adsorbate increases, the adsorption capacity also rises. This phenomenon may be a result of effective collisions between the adsorbate and the adsorbent, which enhanced the adsorption capacity. The obtained results indicate that when employing 100 mg of powdered *D. viscosa* bark powder, the highest adsorption occurs in a 500 ppm solution.

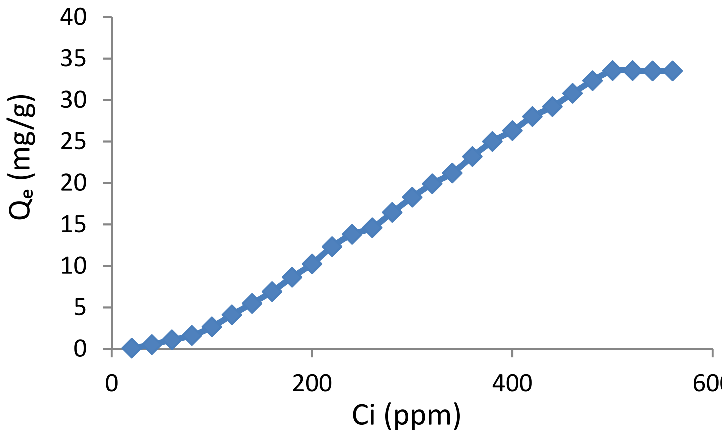

Figure 3. Effect of initial concentration (Ci) of adsorbate on the adsorption of MR dye on *D. viscosa* plant bark.

3.3. Effect of Contact Time on Adsorption

The experiments were conducted under optimized experimental conditions, in order to ascertain how contact duration affects the adsorption process. Eight solutions containing 500 ppm of MR dye, at pH-1, were prepared for this purpose, and 100 mg of bark powder was added to each solution. Each solution's adsorbent–adsorbate contact time ranged from 20 to 105 min. The association between contact time and amount adsorbed is shown in Figure 4. The adsorption capacity of the adsorbent was found to increase with increasing contact time, possibly as a result of the effective collisions and time for the adsorption process to be completed. The comparative analysis of Figures 2–4 helps to identify that the average adsorption capacity of the adsorbent is 35 mg/g.

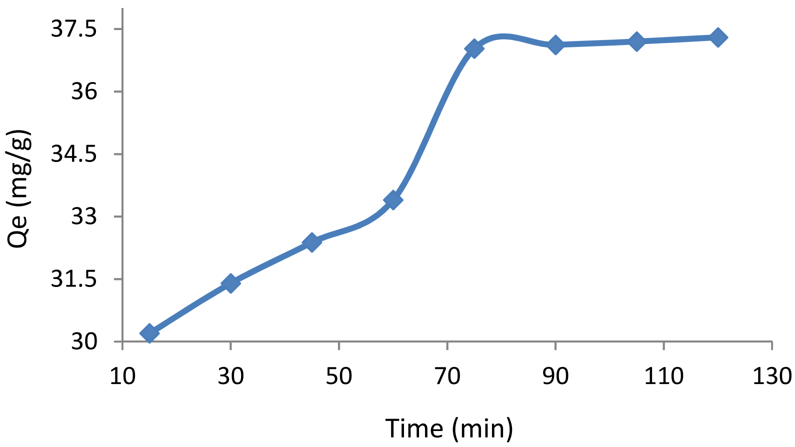

Figure 4. Effect of contact time on the adsorption of MR dyeon *D. viscosa* plant bark.

3.4. Effect of Ionic Strength on Adsorption

To determine the charge on the adsorbent, the impact of ionic strength on the adsorption capacity was observed. To explore the impact of ionic strength, the concentrations of adsorbent, adsorbate, and protons (pH) were kept constant at 100 mg, 500 ppm, and pH = 1, respectively. The concentration of NaCl was changed from 0.1 to 0.9 M. With increasing salt concentration, a reduction in adsorption capacity was seen. Figure 5 depicts the relationship between Qe and molar concentration of NaCl. The findings reveal that the adsorption capacity reduced from 39.9 mg/g to 38.3 mg/g, possibly as a result of the positive charge on the adsorbent's surface because the MR dye has a negative charge. According to the primary salt effect's kinetic phenomenon, a decrease in the rate of the reaction or process occurs when opposite charge carriers contact. This is evidence that the adsorbent's positively charged surface interacts with the negatively charged MR dye through an electrostatic interaction, favoring the high adsorption capacity in an acidic solution.

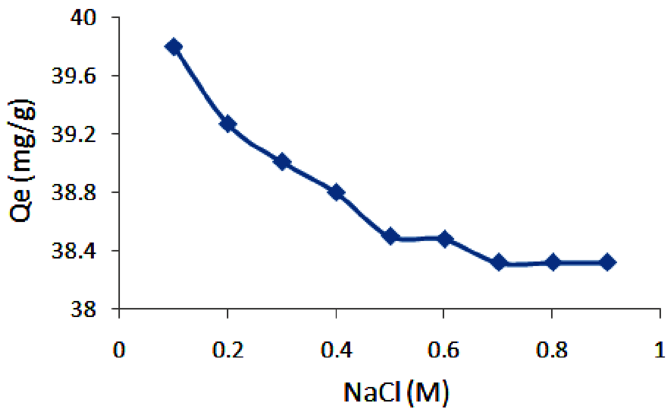

Figure 5. Effect of ionic strength on adsorption of MR dye at *D. viscosa* plant bark powder.

3.5. Effect of Water Obtained from Different Resources on the Adsoprption of MR Dye

While the solutions were being prepared in various aqueous media (i.e., tap water, distilled water, river water, and filtered river water), the MR dye concentration was maintained at 500 ppm, the pH of the solutions was kept at 1, and the contact time for adsorption on a shaker was maintained at 75 min. The percentage of dye removal is shown in all media, on a graph, to assess how different types of water affected equilibrium concentration after adsorption (Figure 6). Filtered river water had the highest level of dye removal at 85.45%, which could be attributed to the best performance of the adsorbent in real water samples rather distilled water.

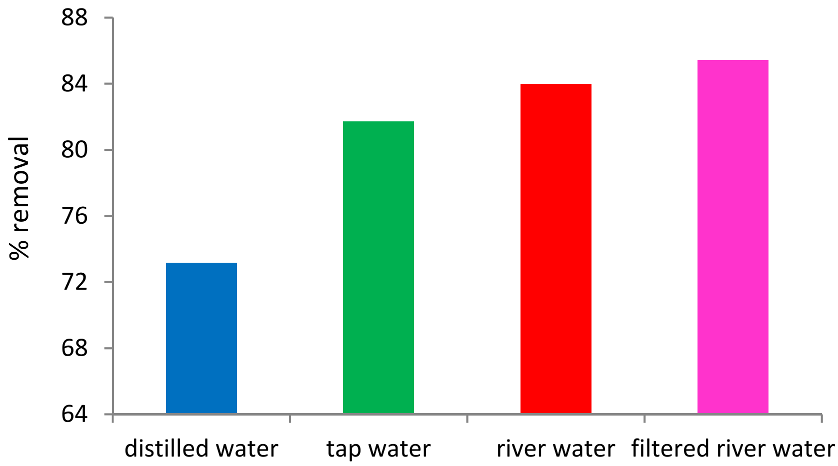

Figure 6. Effect of water collected from different sources on percentage removal of MR dye.

3.6. Comparison between Leaves, Flowers, and Bark Powder of D. viscosa Plant

Three MR dye solutions at 500 ppm concentration, and at pH-1, were made in preparation for the adsorption process, using three various adsorbents. The *D. viscosa* plant's dry and powdered bark, leaves, and flowers served as the adsorbents in this experiment. The purpose of this experiment was to evaluate the ability of other *D. viscosa* plant components to adsorb substances. Observation and calculations show that the bark of the *D. viscosa* plant removes 73% of the MR dye, while the leaves remove 60.8% of the dye and the flowers remove 53.38% of the dye (Figure 7). It was determined that the MR dye had a 36.64 mg/g adsorption capability on the bark of the *D. viscosa* plant. Comparatively, the adsorption capacities for leaves and flowers were determined to be 30.49 mg/g and 26.70 mg/g, respectively.

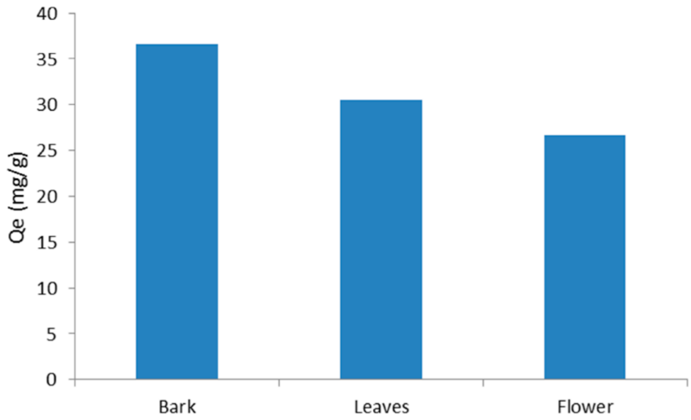

Figure 7. Adsorption of MR dye by bark, leaves, and flowers of *D. viscose* plant.

3.7. Comparison of Adsorbents: Bark Powder of D. viscosa Plant, Animal Charcoal and Silica Gel

To remove MR dye, we compared our chosen adsorbent to other commercially available adsorbents, and we calculated and compared each one's adsorption capacity. The *D. viscosa* plant bark showed a large adsorption capacity of 36.64 mg/g, whereas animal charcoal showed 32.36 mg/g in the form of pellets and 21.59 mg/g in the form of powdered charcoal, and silica gel demonstrated 24.60 mg/g in powder form. This was determined from a comparative analysis of the adsorption capacities of the bark of the *D. viscosa* plant, animal charcoal, and silica gel.

3.8. X-ray Diffraction Analysis

Before and after adsorption, the bark samples were subjected to X-ray diffraction (XRD) examination (Figure 8). Peaks at $2\theta = 15$ show the presence of amorphous hemicelluloses, whereas the peak at $2\theta = 22$ indicates the presence of cellulose in the sample [53–55]. In comparison to the unloaded adsorbent, the MR dye-loaded adsorbent's XRD pattern shows somewhat different peak locations. According to the XRD analyses, the adsorbent's crystallinity has changed as a result of the adsorption process.

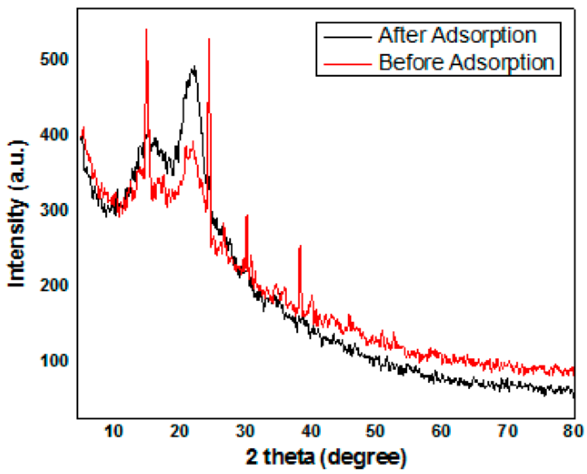

Figure 8. XRD pattern of *D. viscosa* plant bark (adsorbent) before and after adsorption of MR dye.

3.9. Order of Adsorpton Kinetics

To determine the adsorption kinetics, pseudo-first-order (PFO) and pseudo-second-order (PSO) kinetic models were applied to the data (Figure 9). For the adsorption of MR dye on the bark powder of Hopbush, the linear fit shows that the adsorption process follows a PSO kinetics rather than a PFO (Figure 9a,b). When compared to the pseudo-first-order reaction straight line graph, the value of R^2 for the pseudo-second-order reaction straight line graph was found to be relatively near to 1. In light of the findings, a PSO kinetics can be drawn. The pseudo-second-order kinetic model states that the adsorption rate depends on both Qt (adsorption capacity at any time point "t"), and Qe (adsorption capacity at equilibrium) [56]. The following equation illustrates the linear version of the pseudo-second-order adsorption kinetics:

$$t/Qt = 1/k_2Qe^2 + t/Qe \quad (3)$$

where, k_2 denotes the pseudo-second-order rate constant, with dimension g mg^{-1} min^{-1}. A linear plot of t/Qt versus t yields Qe and k_2 (Figure 9b), from the slope and intercept of the plot, respectively. Table 1 displays several parameters derived from the straight-line PFO and PSO graphs' slopes and intercepts. The Qe value is close to the Q_{exp} value, according to the pseudo-second-order kinetic equation.

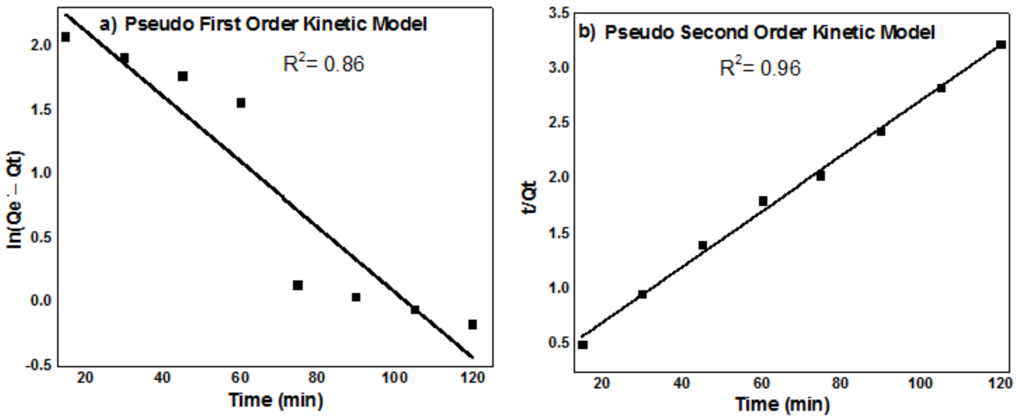

Figure 9. (**a**) Pseudo-first-order kinetic model. (**b**) Pseudo-second-order kinetic model for the adsorption of MR on *D. viscosa* plant bark powder.

Table 1. The kinetic parameters for the adsorption of MR on the *D. viscosa* plant bark powder.

Pseudo First Order Kinetic Model			Pseudo Second Order Kinetic Model		
k_1	Qe	R^2	k_2	Qe	R^2
−0.000213	13.9	0.86341	0.00328	39.75	0.96

3.10. Adsorption Isotherms

The experimental data were examined using Langmuir and Freundlich's adsorption isotherms. Table 2 displays the parameters derived from these isotherms. All adsorbent sites must be equal and the adsorbent surface must be homogenous in order for the Langmuir adsorption isotherm to exist [57]. As a result, the surface of the adsorbent develops a monolayer of adsorbate. The well-known Langmuir equation applied is as follows:

$$Ce/Qe = Ce/Qm + 1/QmK_L \quad (4)$$

Ce is the dye concentration at equilibrium, expressed as ppm, while Qe provides the adsorption capacity at equilibrium, which is defined as the quantity of dye adsorbed per gram of adsorbent (mg g^{-1}). Qm stands for the maximum amount of dye adsorbed per gram of adsorbent (mg g^{-1}). Similarly, K_L stands for the Langmuir adsorption constant. The value 0.694 was the calculated coefficient of determination (R^2) for Langmuir adsorption isotherm, thus indicating that the adsorption behaviour of the examined system does not follow the presumptions of the Langmuir method.

The experimental data were additionally fitted with Freundlich asorption isotherm to take into consideration surface heterogeneity, surface roughness, and the presence of different kinds of adsorption sites. The Freundlich adsorption isotherm has the following linear form:

$$\log Qe = \log K_F + 1/n \log Ce \quad (5)$$

The Freundlich constants K_F and n are related to the capacity and intensity of adsorption, respectively. The linear fit (R^2) value of 0.983 shows that the adsorption process obeys the Freundlich adsorption isotherm. In general, favourable Freundlich adsorption is indicated by n (adsorption intensity) being less than unity. Table 2 displays the values of these constants. According to Table 2, the MR dye adsorption on the bark powder of the *D. viscosa* plant is a physisorption process. It also shows that not all adsorption sites are homogenous, suggesting that multilayer adsorption may take place on the surface of the adsorbent.

Table 2. Adsorption isotherm parameters for the adsorption of MR on *D. viscosa* plant bark.

Adsorbent *D. viscosa* Plant Bark (Powder)	Langmuir Isotherms			Freundlich Isotherm		
	Q_m mg g^{-1}	K_L (Lg^{-1})	R^2	K_F	n	R^2
-	2.53614	−0.00688	0.694	0.00707	0.33664	0.983

3.11. Comparison of Adsorption Capacity of D. viscosa Plant Bark with Previous Low-Cost Adsorbents

Table 3 shows a comparison of *D. viscosa* plant bark powder's ability to adsorb MR dye with that of other inexpensive adsorbents from earlier studies [58–60]. It was discovered through this comparison that utilizing 100 mg of adsorbent per 10 mL of solution MR dye (500 ppm and at pH-1) during a contact time of 75 min offers outstanding results. Additionally, it is notable that this work's adsorbent dose is lower than that of earlier adsorbents and may remove a higher concentration of dye.

Table 3. Comparison of adsorption capacity of the bark powder of Hopbush (*D. viscosa*) with previously studied adsorbents for the removal of MR dye from aqueous solution.

Adsorbents	Adsorbent Dose (mg)	λ_{max} (nm)	pH	Ci (ppm)	Contact Time (min)	Qe (mg/g)	% Removal	Reference
Bark of *D. viscosa*	100	433	1	500	75	36.64	74	Present work
Parkia speciosa Pod	5000	410	-	10	30	-	100	[58]
Pomelo peels	1000	410	6.5	100	80	-	95	[61]
White Potato Peel Powder	1000	-	2	25	80	4.5	90.5	[59]
Bentonite clay	1600	536	2	100	25	-	98.4	[62]
Rice hulls	10,000	-	3	500	100	3.6	65	[63]
Activated carbon prepared from *Annona squmosa* seeds	200	540	4	200	100	27.7	50	[51]

4. Conclusions

This study demonstrates the superior adsorption capacity of *D. viscosa* (Hopbush) plant's bark powder for MR dye removal. Without any chemical treatment, the adsorbent is cost-effectively prepared by washing, drying in sunlight and grinding. The findings showed an overall adsorption capacity of 36.64 mg/g at pH-1, and as a result, this adsorbent may be better able to treat acidic waste water, with a high concentration of dye (500 ppm), within 75 min. The bark of the *D. viscosa* plant has a greater capacity for adsorption than its leaves and flowers. When compared to other adsorbents, however, the adsorption capacity of the leaves and flowers, which is 30.49 mg/g and 26.70 mg/g, respectively, is still rather good. The outcomes also demonstrate that Hopbush bark powder, with a percentage MR dye removal value of 73.15%, has a greater adsorption capacity, when compared to charcoal powder, silica gel powder, and charcoal in the form of pellets, which have values of: 64.72%, 49.06%, and 43.18%, respectively. The high availability, high percentage of dye removal, ease of cultivation, and lack of need for chemical treatment make the bark of the *D. viscosa* plant an efficient, affordable adsorbent. Additionally, the pseudo-second-order kinetic model and the Freundlich adsorption isotherm both accurately depict the MR dye's adsorption process on the bark of the *D. viscosa* plant. Thus, water contamination can be reduced using this natural, inexpensive adsorbent.

Supplementary Materials: The following supporting information can be downloaded at: https://www.mdpi.com/article/10.3390/w14182831/s1, Figure S1: Colour of methyl red at different pH; Figure S2: Protonation of methyl red in acidic solutions; Figure S3: Plot of absorbance as a function of wavelength to determine wavelength maximum (λ_{max}); Explanation E1.

Author Contributions: Conceptualization, S.G., M.K. and H.G.; methodology, S.G., H.G. and R.K.; software, M.K., M.S.K. and A.E.K.; validation, S.G., M.K., R.A.Q., H.G., M.S.K., R.K., F.K. and A.E.K.; formal analysis, M.K., M.S.K. and A.E.K.; investigation, R.K.; resources, S.G. and R.K.; data curation, S.G. and M.K.; writing—original draft preparation, M.K., F.K., H.G. and R.A.Q.; writing—review and editing, R.K., M.S.K. and A.E.K.; visualization, R.A.Q. and R.K.; supervision, S.G.; project administration, S.G. All authors have read and agreed to the published version of the manuscript.

Funding: This research received no external funding.

Data Availability Statement: Not applicable.

Acknowledgments: We acknowledge the Department of Chemistry, Women University Swabi, Pakistan and the Department of Chemistry, Shaheed Benazir Bhutto Women University, Peshawar, Pakistan for financial and technical support.

Conflicts of Interest: The authors declare no conflict of interest.

References

1. Azizullah, A.; Khattak, M.N.K.; Richter, P.; Häder, D.-P. Water pollution in pakistan and its impact on public health—A review. *Environ. Int.* **2011**, *37*, 479–497. [CrossRef] [PubMed]
2. Hinrichsen, D.; Tacio, H. The coming freshwater crisis is already here. In *The Linkages between Population and Water*; Woodrow Wilson International Center for Scholars: Washington, DC, USA, 2002; pp. 1–26.
3. Gupta, V. Application of low-cost adsorbents for dye removal—A review. *J. Environ. Manage.* **2009**, *90*, 2313–2342. [CrossRef]
4. Sudha, M.; Saranya, A.; Selvakumar, G.; Sivakumar, N. Microbial degradation of azo dyes: A review. *Int. J. Curr. Microbiol. Appl. Sci.* **2014**, *3*, 670–690.
5. Hunge, Y.; Mohite, V.; Kumbhar, S.; Rajpure, K.; Moholkar, A.; Bhosale, C. Photoelectrocatalytic degradation of methyl red using sprayed WO_3 thin films under visible light irradiation. *J. Mater. Sci. Mater. Electron.* **2015**, *26*, 8404–8412. [CrossRef]
6. Anjaneyulu, Y.; Sreedhara Chary, N.; Samuel Suman Raj, D. Decolourization of industrial effluents—Available methods and emerging technologies—A review. *Rev. Environ. Sci. Biotechnol.* **2005**, *4*, 245–273. [CrossRef]
7. Kumar, P.S.; Joshiba, G.J.; Femina, C.C.; Varshini, P.; Priyadharshini, S.; Karthick, M.; Jothirani, R. A critical review on recent developments in the low-cost adsorption of dyes from wastewater. *Desalin. Water Treat.* **2019**, *172*, 395–416. [CrossRef]
8. Takkar, S.; Tyagi, B.; Kumar, N.; Kumari, T.; Iqbal, K.; Varma, A.; Thakur, I.S.; Mishra, A. Biodegradation of methyl red dye by a novel actinobacterium *zhihengliuella* sp. Istpl4: Kinetic studies, isotherm and biodegradation pathway. *Environ. Technol. Innov.* **2022**, *26*, 102348. [CrossRef]
9. Patil, N.P.; Bholay, A.D.; Kapadnis, B.P.; Gaikwad, V.B. Biodegradation of model azo dye methyl red and other textile dyes by isolate bacillus circulans npp1. *J. Pure Appl. Microbiol.* **2016**, *10*, 2793–2800. [CrossRef]
10. Vinoda, B.; Vinuth, M.; Bodke, Y.; Manjanna, J. Photocatalytic degradation of toxic methyl red dye using silica nanoparticles synthesized from rice husk ash. *J Environ. Anal. Toxicol.* **2015**, *5*. [CrossRef]
11. Annadurai, G.; Juang, R.-S.; Lee, D.-J. Use of cellulose-based wastes for adsorption of dyes from aqueous solutions. *J. Hazard. Mater.* **2002**, *92*, 263–274. [CrossRef]
12. Ahmad, M.A.; Ahmad, N.; Bello, O.S. Modified durian seed as adsorbent for the removal of methyl red dye from aqueous solutions. *Appl. Water Sci.* **2015**, *5*, 407–423. [CrossRef]
13. Rajoriya, S.; Saharan, V.K.; Pundir, A.S.; Nigam, M.; Roy, K. Adsorption of methyl red dye from aqueous solution onto eggshell waste material: Kinetics, isotherms and thermodynamic studies. *Curr. Res. Green Sustain. Chem.* **2021**, *4*, 100180. [CrossRef]
14. Xiang, P.; Deng, C.; Liu, L.; Huang, Y. *Study on the Adsorption of Methyl Red by Bentonite/Chitosan Composites. InIOP Conference Series: Materials Science and Engineering*; IOP Publishing: Bristol, UK, 2020; p. 022079.

15. Dawadi, K.B.; Bhattarai, M.; Homagai, P.L. Adsorptive removal of methyl red from aqueous solution using charred and xanthated sal (*Shorea robusta*) sawdust. *Amrit Res. J.* **2020**, *1*, 37–44. [CrossRef]
16. Santhi, T.; Manonmani, S.; Smitha, T. Removal of malachite green from aqueous solution by activated carbon prepared from the epicarp of ricinus communis by adsorption. *J. Hazard. Mater.* **2010**, *179*, 178–186. [CrossRef] [PubMed]
17. Mahmoud, N.A.; Nassef, E.; Husain, M. Use of spent oil shale to remove methyl red dye from aqueous solutions. *AIMS Mater. Sci.* **2020**, *7*, 338–353. [CrossRef]
18. Adeniyi, A.G.; Ighalo, J.O. Biosorption of pollutants by plant leaves: An empirical review. *J. Environ. Chem. Eng.* **2019**, *7*, 103100. [CrossRef]
19. Anastopoulos, I.; Robalds, A.; Tran, H.N.; Mitrogiannis, D.; Giannakoudakis, D.A.; Hosseini-Bandegharaei, A.; Dotto, G.L. Removal of heavy metals by leaves-derived biosorbents. *Environ. Chem. Lett.* **2019**, *17*, 755–766. [CrossRef]
20. Anastopoulos, I.; Bhatnagar, A.; Bikiaris, D.N.; Kyzas, G.Z. Chitin adsorbents for toxic metals: A review. *Int. J. Mol. Sci.* **2017**, *18*, 114. [CrossRef]
21. Babatunde, E.; Akolo, S.; Ighalo, J.; Kovo, A. Response Surface Optimisation of the Adsorption of Cu (ii) from Aqueous Solution by Crab Shell Chitosan. In Proceedings of the 3rd International Engineering Conference, Minna, Nigeria, 24–26 September 2019.
22. An, H.; Park, B.; Kim, D. Crab shell for the removal of heavy metals from aqueous solution. *Water Res.* **2001**, *35*, 3551–3556. [CrossRef]
23. Babarinde, A.; Onyiaocha, G.O. Equilibrium sorption of divalent metal ions onto groundnut (*Arachis hypogaea*) shell: Kinetics, isotherm and thermodynamics. *Chem. Int.* **2016**, *2*, 37–46.
24. Olakunle, M.O.; Inyinbor, A.A.; Dada, A.O.; Bello, O.S. Combating dye pollution using cocoa pod husks: A sustainable approach. *Int. J. Sustain. Eng.* **2018**, *11*, 4–15. [CrossRef]
25. Series, I.; Science, M. Utilization of cacao pod husk (*Theobroma cacao* L.) as activated carbon and catalyst in biodiesel production process from waste cooking oil. In *IOP Conference Series: Materials Science and Engineering*; IOP Publishing: Bristol, UK, 2018; p. 012093.
26. Mutavdžić Pavlović, D.; Ćurković, L.; Macan, J.; Žižek, K. Eggshell as a new biosorbent for the removal of pharmaceuticals from aqueous solutions. *CLEAN–Soil Air Water* **2017**, *45*, 1700082. [CrossRef]
27. Bamukyaye, S.; Wanasolo, W. Performance of egg-shell and fish-scale as adsorbent materials for chromium(VI) removal from effluents of tannery industries in eastern uganda. *Open Access Lib. J.* **2017**, *4*, 1–12. [CrossRef]
28. Hevira, L.; Munaf, E.; Zein, R. The use of *Terminalia catappa* L. Fruit shell as biosorbent for the removal of Pb(II), Cd(II) and Cu(II) ion in liquid waste. *J. Chem. Pharm. Res.* **2015**, *7*, 79–89.
29. Sud, D.; Mahajan, G.; Kaur, M. Agricultural waste material as potential adsorbent for sequestering heavy metal ions from aqueous solutions—A review. *Bioresour. Technol.* **2008**, *99*, 6017–6027. [CrossRef] [PubMed]
30. Petrović, M.; Šoštarić, T.; Stojanović, M.; Milojković, J.; Mihajlović, M.; Stanojević, M.; Stanković, S. Removal of Pb^{2+} ions by raw corn silk (*Zea mays* L.) as a novel biosorbent. *J. Taiwan Inst. Chem. Eng.* **2016**, *58*, 407–416. [CrossRef]
31. Petrović, M.; Šoštarić, T.; Stojanović, M.; Petrović, J.; Mihajlović, M.; Ćosović, A.; Stanković, S. Mechanism of adsorption of Cu^{2+} and Zn^{2+} on the corn silk (*Zea mays* L.). *Ecol. Eng.* **2017**, *99*, 83–90. [CrossRef]
32. Eletta, O.A.; Ighalo, J.O. A review of fish scales as a source of biosorbent for the removal of pollutants from industrial effluents. *J. Res. Inf. Civ. Eng.* **2019**, *16*, 2479–2510.
33. Ahmadifar, Z.; Dadvand Koohi, A. Characterization, preparation, and uses of nanomagnetic fe3o4 impregnated onto fish scale as more efficient adsorbent for Cu^{2+} ion adsorption. *Environ. Sci. Pollut. Res.* **2018**, *25*, 19687–19700. [CrossRef]
34. Ribeiro, C.; Scheufele, F.; Alves, H.; Kroumov, A.; Espinoza-Quiñones, F.; Módenes, A.; Borba, C. Evaluation of hybrid neutralization/biosorption process for zinc ions removal from automotive battery effluent by dolomite and fish scales. *Environ. Technol.* **2019**, *40*, 2373–2388. [CrossRef]
35. Olasehinde, E.F.; Okoronkwo, A.E.; Aiyesanmi, A.F. Biosorption of nickel from aqueous solution by tithonia diversifolia. *Desalination Water Treat.* **2009**, *12*, 352–359.
36. Sekar, M.; Sakthi, V.; Rengaraj, S. Kinetics and equilibrium adsorption study of lead(II) onto activated carbon prepared from coconut shell. *J. Colloid Interface Sci.* **2004**, *279*, 307–313. [CrossRef]
37. Al-Othman, Z.A.; Ali, R.; Naushad, M. Hexavalent chromium removal from aqueous medium by activated carbon prepared from peanut shell: Adsorption kinetics, equilibrium and thermodynamic studies. *Chem. Eng. J.* **2012**, *184*, 238–247. [CrossRef]
38. Romzi, A.A.; Kooh, M.R.R.; Lim, L.B.L.; Priyantha, N.; Chan, C.M. Environmentally friendly adsorbent derived from rock melon skin for effective removal of toxic brilliant green dye: Linear versus non-linear analyses. *Int. J. Environ. Anal. Chem.* **2021**, 1–20. [CrossRef]
39. Petrović, J.T.; Stojanović, M.D.; Milojković, J.V.; Petrović, M.S.; Šoštarić, T.D.; Laušević, M.D.; Mihajlović, M.L. Alkali modified hydrochar of grape pomace as a perspective adsorbent of pb^{2+} from aqueous solution. *J. Environ. Manag.* **2016**, *182*, 292–300. [CrossRef] [PubMed]
40. Şen, A.; Pereira, H.; Olivella, M.; Villaescusa, I. Heavy metals removal in aqueous environments using bark as a biosorbent. *Int. J. Environ. Sci. Tech.* **2015**, *12*, 391–404. [CrossRef]
41. Afroze, S.; Sen, T.K.; Ang, H. Adsorption performance of continuous fixed bed column for the removal of methylene blue (MB) dye using eucalyptus sheathiana bark biomass. *Res. Chem. Intermed.* **2016**, *42*, 2343–2364. [CrossRef]

42. Afroze, S.; Sen, T.K.; Ang, H.M. Adsorption removal of zinc(II) from aqueous phase by raw and base modified eucalyptus sheathiana bark: Kinetics, mechanism and equilibrium study. *Process Saf. Environ. Prot.* **2016**, *102*, 336–352. [CrossRef]
43. AREMU, M.O.; Alade, A.; Bello, A.; Salam, K. Kinetics and thermodynamics of 2, 4, 6–trichlorophenol adsorption onto activated carbon derived from flamboyant pod bark. *J. Int. Environ. Appl. Sci.* **2018**, *13*, 158–166.
44. Ajaelu, C.J.; Nwosu, V.; Ibironke, L.; Adeleye, A. Adsorptive removal of cationic dye from aqueous solution using chemically modified african border tree (*Newbouldia laevis*) bark. *J. Appl. Sci. Environ. Manag.* **2017**, *21*, 1323–1329. [CrossRef]
45. Cutillas-Barreiro, L.; Ansias-Manso, L.; Fernández-Calviño, D.; Arias-Estévez, M.; Nóvoa-Muñoz, J.; Fernández-Sanjurjo, M.; Álvarez-Rodríguez, E.; Núñez-Delgado, A. Pine bark as bio-adsorbent for cd, cu, ni, pb and zn: Batch-type and stirred flow chamber experiments. *J. Environ. Manag.* **2014**, *144*, 258–264. [CrossRef] [PubMed]
46. Cong, L.; Feng, L.; Wei, X.; Jin, J.; Wu, K. Study on the adsorption characteristics of congo red by sycamore bark activated carbon. In environment. technologies. resources. In Proceedings of the International Scientific and Practical Conference, Kharkov, Ukraine, 10–13 October 2017; pp. 64–69.
47. Kooh, M.R.R.; Thotagamuge, R.; Chau, Y.-F.C.; Mahadi, A.H.; Lim, C.M. Machine learning approaches to predict adsorption capacity of azolla pinnata in the removal of methylene blue. *J. Taiwan Inst. Chem. Eng.* **2022**, *132*, 104134. [CrossRef]
48. Eletta, O.; Ayandele, F.; Adeniyi, A.; Ighalo, J. Valorisation of sunflower (*Tithonia diversifolia*) stalks for the adsorption of Pb(II) and Fe(II) from aqueous media. *NSChE J.* **2020**, *35*, 107.
49. Ighalo, J.O.; Adeniyi, A.G. Adsorption of pollutants by plant bark derived adsorbents: An empirical review. *J. Water Process Eng.* **2020**, *35*, 101228. [CrossRef]
50. Al-Snafi, A.E. Traditional uses of iraqi medicinal plants. *IOSR J. Pharm.* **2018**, *8*, 32–96.
51. Santhi, T.; Manonmani, S.; Smitha, T. Removal of methyl red from aqueous solution by activated carbon prepared from the annona squmosa seed by adsorption. *Chem. Eng. Res. Bull.* **2010**, *14*, 11–18. [CrossRef]
52. Dragan, E.S.; Dinu, I.A. Interaction of dis-azo dyes with quaternized poly (dimethylaminoethyl methacrylate) as a function of the dye structure and polycation charge density. *J. Appl. Polymer Sci.* **2009**, *112*, 728–735. [CrossRef]
53. Elabed, A.; Saoiabi, A.P. Réactivité Thermique et Cinétique de Dégradation du Bois d'Arganier: Application à l'Élaboration du Charbon Actif par Activation Chimique à l'Acide Phosphorique. Ph.D. Thesis, Université Mohammed V-AGDAL, Rabat, Morocco, 2007.
54. Essaadaoui, Y.; Lebkiri, A.; Rifi, E.H.; Kadiri, L.; Ouass, A. Adsorption of cobalt from aqueous solutions onto bark of eucalyptus. *Mediterr. J. Chem.* **2018**, *7*, 145–155. [CrossRef]
55. Murtaza, G.; Zia, M.H. Wastewater production, treatment and use in pakistan. In Proceedings of the Second Regional Workshop of the Project 'Safe Use of Wastewater in Agriculture, New Delhi, India, 16–18 May 2012; pp. 16–18.
56. Naeem, H.; Ajmal, M.; Muntha, S.; Ambreen, J.; Siddiq, M. Synthesis and characterization of graphene oxide sheets integrated with gold nanoparticles and their applications to adsorptive removal and catalytic reduction of water contaminants. *RSC Adv.* **2018**, *8*, 3599–3610. [CrossRef]
57. Zhang, X.; Liu, J.; Kelly, S.J.; Huang, X.; Liu, J. Biomimetic snowflake-shaped magnetic micro-/nanostructures for highly efficient adsorption of heavy metal ions and organic pollutants from aqueous solution. *J. Mater. Chem. A* **2014**, *2*, 11759–11767. [CrossRef]
58. Mohamad, R.; Alias, M.Z.M.; Ghazi, R.M. Removal of methyl red using chemical impregnated activated carbon prepared from parkia speciosa pod (petai) as a potential adsorbent. *J. Trop. Resour. Sustain. Sci. (JTRSS)* **2017**, *5*, 62–65. [CrossRef]
59. Enenebeaku, C.K.; Okorocha, N.J.; Uchechi, E.E.; Ukaga, I.C. Adsorption and equilibrium studies on the removal of methyl red from aqueous solution using white potato peel powder. *Int. Lett. Chem. Phys. Astron.* **2017**, *72*, 52. [CrossRef]
60. Ahmad, M.A.; Ahmed, N.A.B.; Adegoke, K.A.; Bello, O.S. Sorption studies of methyl red dye removal using lemon grass (*Cymbopogon citratus*). *Chem. Data Collect.* **2019**, *22*, 100249. [CrossRef]
61. Tanzim, K.; Abedin, M.Z. A novel bioadsorbent for the removal of methyl red from aqueous solutions. *IOSR J. Environ. Sci. Toxicol. Food Technol.* **2015**, *9*, 87–91.
62. Fosso-Kankeu, E.; Webster, A.; Ntwampe, I.; Waanders, F. Coagulation/flocculation potential of polyaluminium chloride and bentonite clay tested in the removal of methyl red and crystal violet. *Arab. J. Sci. Eng.* **2017**, *42*, 1389–1397. [CrossRef]
63. Abdulhussein, H.A.; Hassan, A.A. Methyl red dye removal from aqueous solution by adsorption on rice hulls. *Babylon Univ. Sci.* **2015**, *23*, 627–637.